

# Sucrose Hydrates in Aqueous Solution by IR Spectroscopy

Jean-Joseph Max<sup>†</sup> and Camille Chapados\*

Département de chimie-biologie, Université du Québec à Trois-Rivières, Trois-Rivières, QC, Canada G9A 5H7

Received: July 23, 2001; In Final Form: September 5, 2001

Two sucrose hydrates were found by factor analysis (FA) of the mid-infrared attenuated total reflectance (MIR-ATR) spectra of a series of aqueous sucrose solutions: sucrose penta- and dihydrate. The spectra of the isolated hydrates and their abundances as a function of concentration were obtained. Apart from the intensity of the water bands, the two hydrates differ only in a few sucrose bands in the C–O region. From the distribution of the species, the equilibrium between penta- and dihydrate was deduced:  $3\text{H}_2\text{O} + \text{C}_{12}\text{H}_{22}\text{O}_{11} \cdot 2\text{H}_2\text{O} \rightleftharpoons \text{C}_{12}\text{H}_{22}\text{O}_{11} \cdot 5\text{H}_2\text{O}$ . The pentahydrate equilibrium constant was found to be  $K_e = (4.1 \pm 0.3) \times 10^{-5} \text{ L}^3 \text{ mol}^{-3}$ . The two hydrates observed in aqueous solution are not found in the solid state. Analysis of the integrated intensity of the OH stretching band of sucrose–H<sub>2</sub>O mixtures shows that the OH vibrations in both the sucrose and the associated water are modified in the mixtures, indicating strong intermolecular interactions that influence the band intensities.

## 1. Introduction

Because of the commercial importance of sucrose (C<sub>12</sub>H<sub>22</sub>O<sub>11</sub>), its conformation in water has been studied extensively. Based on thermodynamic data from the 1920s, aqueous sucrose solutions were thought to contain a hexahydrate at moderate concentrations.<sup>1,2</sup> More recently, a sucrose monohydrate was discovered by molecular dynamics simulation.<sup>3,4</sup> Several infrared (IR) and Raman studies of aqueous sucrose were reported: (1) some dealt with the conformational arrangement and the equilibrium of different sugar anomers;<sup>5–7</sup> (2) others dealt with the quantitative analysis of sugar in different aqueous media.<sup>7–15</sup> Some of these studies showed linearity only over a limited concentration range.<sup>9–10,12,15</sup> In none, however, was there a clear determination of the exact sucrose composition in aqueous solutions.

IR spectroscopy is a technique whereby various species in a mixture can be identified and their abundances determined.<sup>7–29</sup> Because the OH stretch vibrations are strong absorbers, transmission IR measurements of aqueous solutions are difficult to obtain.<sup>30</sup> On the other hand, attenuated total reflectance (ATR) allows a quantitative determination of the complete mid-IR (MIR) spectrum of an aqueous system.<sup>5,8,10,12,14–27</sup> We have developed an adequate quantitative method with ATR that provides reliable results consistently as long as the following basic requirements are met: (1) a proper crystal is used whose refractive index is sufficiently different from that of the solution;<sup>17</sup> (2) the IR beam is at a proper angle of incidence; (3) the ATR crystal is of adequate length. When these conditions are satisfied, the IR-ATR spectra reflect the system's chemical composition.<sup>17</sup> Using this technique, several aqueous solutions of alkali halides were analyzed and several acid–base titrations were made. We found that water forms stable clusters with the ions when a binary salt (NaCl, KCl), a strong acid (HCl), or a strong base (NaOH) is dissolved in it.<sup>18–21,25,27,29</sup> By this

technique, we detected the formation of complexes in aqueous sulfuric and phosphoric acids.<sup>23–24,26</sup> Some of these complexes were previously found only from thermodynamic measurements.

We have applied principal factor analysis (FA) in the past to a series of IR spectra in order to determine the abundance of the species and to obtain their spectra. This is a suitable type of analysis when some of the species can be obtained easily from the set of experimental spectra. Other FA methods can be used<sup>31</sup> that yield either abstract spectra<sup>6,8,14</sup> or, under more demanding conditions, real spectra.<sup>28,32</sup>

The purpose of the present study is to analyze the MIR spectra of aqueous sucrose solutions over the entire solubility range. Specifically, we want to determine: (i) the number of species present in the solutions; (ii) the species abundances; (iii) the MIR spectra of sucrose hydrates; (iv) the molecular composition of the hydrates.

## 2. Experimental Methods and Data Analysis

**2.1. Chemicals and Solutions.** Sucrose (Aldrich Chemical Co., A. C. S. reagent [57-50-1], purity >99%, water content <0.03%, FW. 342.30) was used without further purification. Deionized water was used to prepare the aqueous solutions. Each sample was prepared by first weighing dried sucrose in an empty 10 mL volumetric flask, completing the volume with water, and then weighing it again. A series of 18 samples ranging from 0 to 2.628 M (899.5 g/L) of sucrose were prepared (see Table 1). To allow equilibrium to be reached between species, all samples were prepared several hours before recording the IR spectra.

**2.2. IR Measurements.** The IR measurements were obtained using a model 510P Nicolet FT-IR spectrometer with a TGS detector. Two KBr windows isolated the measurement chamber from the outside. The samples were contained in a Circle cell (SpectraTech, Inc.) equipped with a ZnSe crystal rod (8 cm long) in an ATR configuration (the beam is incident at an angle of 45° with the rod's axis and makes 11 internal reflections). The spectral range of the ZnSe rod is 6500 to 650 cm<sup>-1</sup>. The spectra were taken under a nitrogen flow to ensure low CO<sub>2</sub> and water vapor residues in the spectrometer. Each spectrum represents

\* Corresponding author. Département de chimie-biologie, Université du Québec à Trois-Rivières, C. P. 500, Trois-Rivières, QC, Canada G9A 5H7. E-mail: Camille\_Chapados@uqtr.ca.

<sup>†</sup> Current address: Sciencetech R&D, 247 Thibeau, Cap-de-la-Madeleine, (QC), Canada G8Y 6X9.

**TABLE 1: Parameter of the Experimental Aqueous Sucrose Mixtures (FW (C<sub>12</sub>H<sub>22</sub>O<sub>11</sub>) = 342.30)**

sample composition				final MFs		
sucrose		water		sucrose hydrate II	sucrose hydrate I	water
g L <sup>-1</sup>	mol L <sup>-1</sup>	g L <sup>-1</sup>	mol L <sup>-1</sup>			
0.0	0.000	997.0	55.34	0.000	0.000	1.000
2.0	0.006	996.0	55.29	0.000	0.003	0.998
3.1	0.009	995.3	55.25	0.000	0.005	0.997
5.1	0.015	994.5	55.20	0.000	0.007	0.994
10.1	0.029	991.5	55.04	0.000	0.012	0.993
19.9	0.058	985.8	54.72	0.002	0.023	0.983
29.9	0.087	978.2	54.23	0.003	0.034	0.974
40.4	0.118	972.0	53.96	0.004	0.046	0.965
49.9	0.146	965.6	53.60	0.008	0.053	0.959
99.9	0.292	933.2	51.80	0.018	0.105	0.915
199.5	0.583	870.5	48.32	0.051	0.197	0.829
300.2	0.877	811.3	45.03	0.104	0.269	0.747
400.0	1.168	746.7	41.45	0.174	0.326	0.666
499.6	1.460	684.0	37.97	0.265	0.362	0.582
599.9	1.753	619.7	34.40	0.388	0.369	0.506
699.9	2.045	557.9	30.97	0.541	0.338	0.439
800.0	2.337	494.8	27.47	0.732	0.268	0.376
899.5	2.628	433.8	24.07	0.912	0.176	0.336

an accumulation of 500 scans at 4 cm<sup>-1</sup> resolution. All measurements were taken at 26.5 ± 0.3 °C. The cell was carefully washed and dried before each measurement. Model 510P is a single-beam spectrometer, and a background spectrum was recorded with the cell empty before the measurement of each sample.

The IR measurements consisted in obtaining the ATR background intensity,  $R_0$ , and the ATR sample intensity,  $R$ . The ratio of  $R/R_0$  is the intensity  $I$  for the spectral range being studied. Thereafter, the 3034 data points  $\{I(\tilde{\nu}) \text{ vs } \tilde{\nu} \text{ (in cm}^{-1}\text{)}\}$  of each spectrum were transferred to a spreadsheet program for numerical analysis. Next, the intensities  $I$  were transformed to absorbance,  $\log(1/I)$ . A small baseline shift (less than 0.01 au) was made to obtain a null mean absorbance in the 6000–5500 cm<sup>-1</sup> region where water<sup>30</sup> and sucrose do not absorb. Second derivatives were calculated by the Savitzky and Golay method<sup>33</sup> with a moving quadratic-cubic polynomial fitting on 11 successive data points.

**2.3. Factor Analysis (FA).** Factor analysis of a spectral data set is a process by which the principal species of a mixture can be identified and their concentrations obtained through calibration of derived multiplying factors (MFs). Direct FA is performed on the solution spectra by starting with two known spectra. Pure water is obviously a pure species and makes up the first principal factor. Pure sucrose is a solid and cannot be used directly, so a concentrated sucrose solution was taken as the second principal factor. FA was performed on a personal computer with a spreadsheet program using the following iterative procedure:<sup>18,24</sup> (1) water and concentrated aqueous sucrose are used as principal spectra; (2) a set of realistic MFs are chosen with which to multiply the principal spectra and form a sum ( $\sum (\text{MF} \times \text{principal spectra})$ ); (3) the sums are then compared to the experimental spectra and the resulting residues minimized in accordance with a least-squares fit procedure; (4) the presence of nonzero residues serves to identify another principal spectrum that is then added to the previous principal spectra, and the procedure is repeated from step 1 until the residues were minimized. With the number of factors in the system now determined, these final MFs are multiplied by the sample principal spectra concentrations to give the species concentrations. The presence of negative or inadequate concentrations is taken as a sign that the principal spectra are not orthogonal; an adequate procedure is used to render them

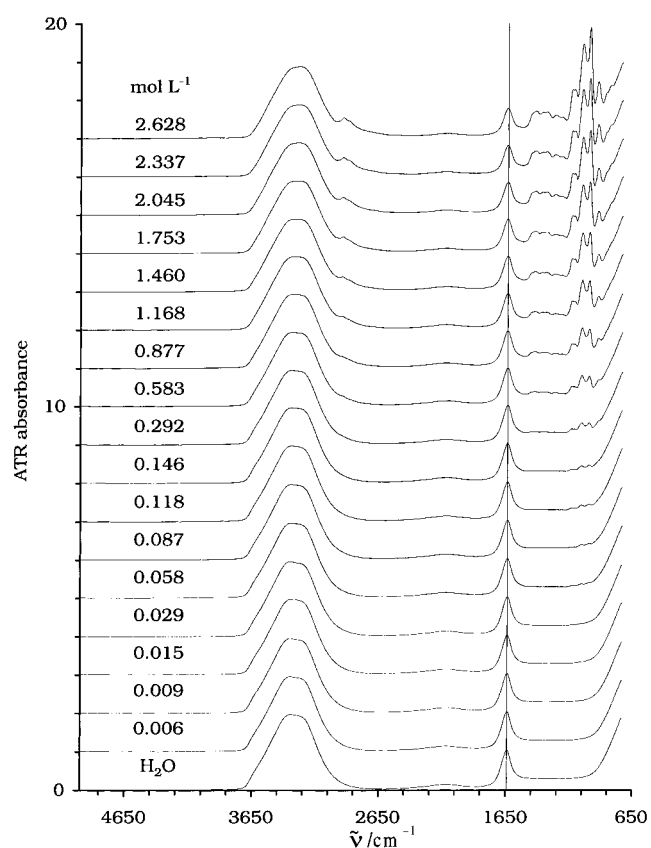


**Figure 1.** Experimental ATR-IR spectra of 18 mixtures of sucrose and water. The bottom spectrum is that of pure water; the others are successively displaced by 1 au. The vertical line is situated at 1638 cm<sup>-1</sup>.

orthogonal. The final MFs are then obtained, and the orthogonal principal spectra (eigenspectra) and final concentrations are determined.

### 3. Results and Discussion

**3.1. Experimental ATR Spectra.** *3.1.1. The Spectra.* The 18 experimental ATR spectra presented in Figure 1 illustrate the effects of gradually increasing the sucrose concentration. Pure water (bottom spectrum) has a broad intense  $\nu_{1,3}$  band from

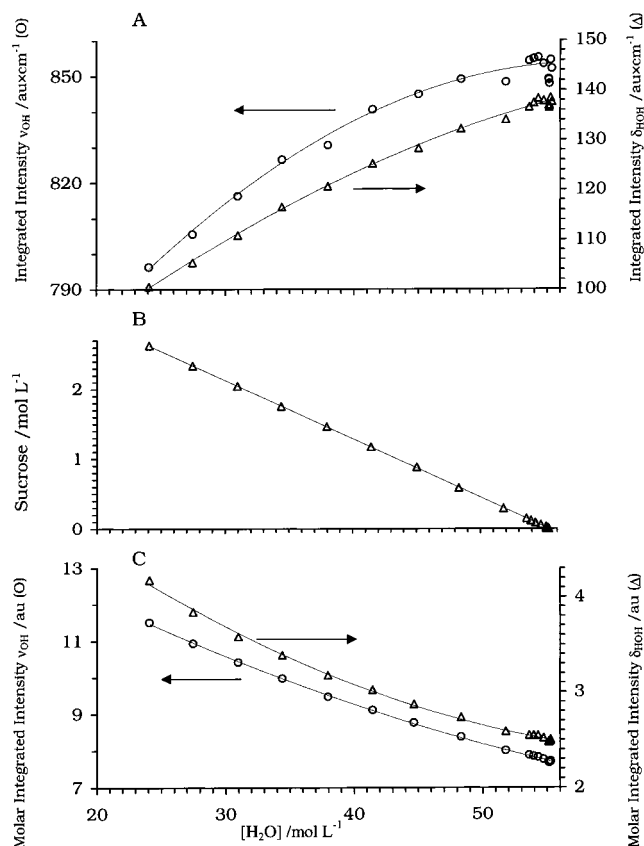


**Figure 2.** Variation against the water concentration of: (A) experimental integrated intensities of sucrose solutions  $\nu_{\text{OH}}$  (O, left scale),  $\delta_{\text{HOH}}$  ( $\Delta$ , right scale), and calculated intensities (full lines); (B) sucrose concentration; and (C) molar integrated intensities (in  $\text{au} \times \text{cm}^{-1}/(\text{mol OH}) \text{L}^{-1}$ ) of  $\nu_{\text{OH}}$  (O, left scale),  $\delta_{\text{HOH}}$  ( $\Delta$ , right scale), and calculated intensities (full lines). Note: the arrows point toward the ordinate scales.

3000 to 3600  $\text{cm}^{-1}$ , a  $\nu_2$  band at 1638  $\text{cm}^{-1}$  (indicated by the vertical line), and a weak broad combination band at 2115  $\text{cm}^{-1}$ . Libration bands of water below 650  $\text{cm}^{-1}$  produce the strong absorption that starts near 1000  $\text{cm}^{-1}$ .<sup>34</sup> The spectrum of the most concentrated sucrose solution is seen at the top in Figure 1. Salient features are the C–H stretching modes in the 2700–3000  $\text{cm}^{-1}$  region, intense bands in the 1000  $\text{cm}^{-1}$  region due to the C–O and C–C stretch vibrations, and a broad band near 1400  $\text{cm}^{-1}$  produced by the C–C–H and C–O–H deformation modes. Increasing the sucrose concentration makes for stronger bands generally, but the two intense bands near 1000  $\text{cm}^{-1}$  do not follow the same pattern: one component grows stronger than the other (Figure 1). This variation suggests that more than one sucrose species is present in the solutions.

**3.1.2. Integrated Intensity of O–H Vibrations in Aqueous Sucrose.** Figure 2A shows the integrated intensities as a function of water concentration of the OH stretch vibration,  $\nu_{\text{OH}}$  (O, left scale) and HOH deformation,  $\delta_{\text{HOH}}$  ( $\Delta$ , right scale) in the 3700–3000  $\text{cm}^{-1}$  and 1750–1500  $\text{cm}^{-1}$  regions, respectively. The two curves display a nonlinear variation. Both water and sucrose contribute to the integrated  $\nu_{\text{OH}}$  intensity.

Figure 2B, a plot of the sucrose concentration as a function of water concentration, illustrates the linear relationship between the two substances in the solutions, that is:

$$c_s = c_0 - ac_w \quad (1)$$

where  $c_s$  and  $c_w$  (mol/L) are the sucrose and water concentrations, respectively. From the figure, we obtain that  $c_0 = 4.643$  mol/L and  $a = 0.084$ . Equation 1 indicates that one sucrose

molecule takes the place of  $1/0.084 = 11.9$  water molecules. Furthermore, the maximum sucrose concentration (when no water is present, i.e.,  $c_w = 0$ ) is equal to 4.643 mol/L, which corresponds to a density of  $4.643 \times 342.3 = 1589$  g/L. This value is slightly higher (0.5%) than the density of crystalline sucrose at 17.5 °C,<sup>35</sup> indicating that packing in both substances is similar.

The  $\nu_{\text{OH}}$  integrated intensity (Figure 2A) in a sample spectrum depends on both water and sucrose contributions. Therefore,

$$\int_{\nu_{\text{OH}}}^{\text{sample}} I(\nu) d\nu = c_w \int_{\nu_{\text{OH}}}^{\text{water}} I(\nu) d\nu + c_s \int_{\nu_{\text{OH}}}^{\text{sucrose}} I(\nu) d\nu \quad (2)$$

where the superscript identifies the molecule that contributes to the integrated intensity. Assuming that the molar contributions of water and sucrose to the integrated intensity of the absorption band are unchanged in a mixture, we combine eqs 1 and 2:

$$\int_{\nu_{\text{OH}}}^{\text{sample}} I(\nu) d\nu = c_0 \int_{\nu_{\text{OH}}}^{\text{sucrose}} I(\nu) d\nu + c_w \left\{ \int_{\nu_{\text{OH}}}^{\text{water}} I(\nu) d\nu - a \int_{\nu_{\text{OH}}}^{\text{sucrose}} I(\nu) d\nu \right\} \quad (3)$$

Because  $c_0$  and  $a$  are constants, eq 3 would suggest that the OH stretch band integrated intensity is proportional to the water concentration. However, we see in Figure 2A (O, left scale) that this is not the case. We conclude from this that the water and sucrose  $\nu_{\text{OH}}$  intensities are perturbed when these two substances are mixed. Similar results were found for the deformation band of water,  $\delta_{\text{HOH}}$ , (Figure 2A:  $\Delta$ , right scale), although sucrose makes no contribution to this band. The mean OH molar integrated intensities as a function of water concentration are plotted in Figure 2C (left scale for the stretch vibrations (O); right scale for the deformation vibrations ( $\Delta$ )).

**3.2. Subtraction of the First Principal Factor.** We have previously reported quantitative subtraction of the water spectrum in aqueous systems using the water bands as indicators provided that no negative band is produced in the process.<sup>18–21,23–27</sup> However, the overlapping of the  $\nu_{\text{OH}}$  bands of water and sucrose in the present case (Figure 1) renders subtraction of the water spectrum more difficult. To facilitate water spectral subtraction, we utilized all of the following indicators: (1) the combination band  $\nu_2 + \nu_L$  near 2115  $\text{cm}^{-1}$ , a broad and weak band that introduces some uncertainty in the subtracted spectra; (2) the deformation band of water  $\nu_2$  near 1638  $\text{cm}^{-1}$  can be used, but only in a limited way since it overlaps with the neighboring absorption; (3) the second derivative technique can be used only as a supplement because it is not very effective in reducing the bandwidth of the very broad water bands.<sup>29</sup> The use of all these techniques allowed us to subtract the spectrum of water from those of the mixtures.

The spectra obtained after water subtraction are shown in Figure 3 (note that the intensity scale is increased by the factor given in the column on the right). Even after the water spectrum is reduced to a minimum, the spectra still show an absorption band near 1640  $\text{cm}^{-1}$  (vertical line in the figure). This band can only be assigned to water since sucrose does not absorb in this region; it also suggests that water different from pure water is associated with sucrose to form sucrose hydrates. In the C–O region of Figure 3 (near 1000  $\text{cm}^{-1}$ ), we observe a variation in the intensity ratio between the 1045 and 993  $\text{cm}^{-1}$  bands as the sucrose concentration increases. This indicates that at least two sucrose hydrates are present in the solutions. At this stage we have subtracted too much pure water. This over subtraction will be clear later on when we correct for this artifact; it did not prevent FA from proceeding correctly, however.

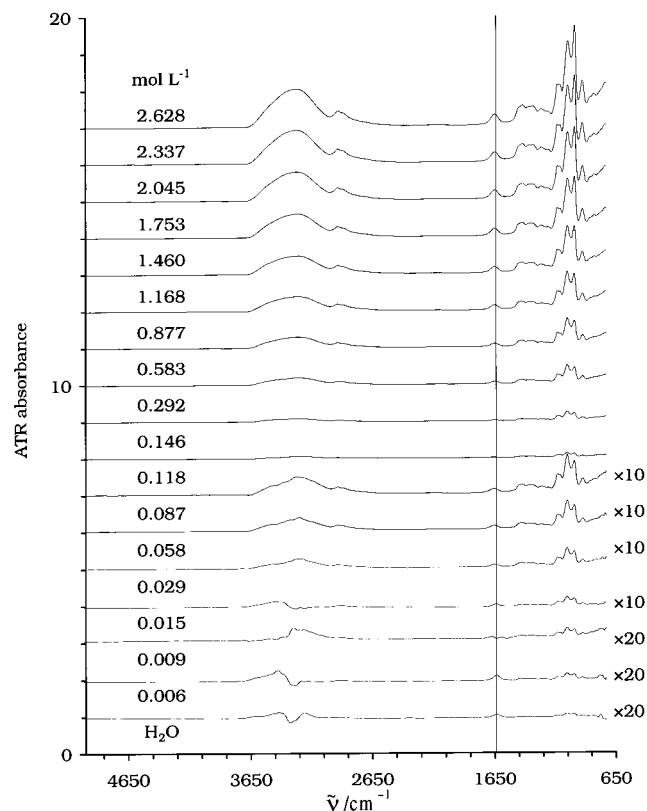


**Figure 3.** Sucrose solutions spectra of Figure 1 after maximum water spectral subtraction. Same display as in Figure 1. For the concentrations 0 to 0.015 mol/L (scale  $\times 20$ ) and 0.029 to 0.118 mol/L (scale  $\times 10$ ).

**3.3. Subtraction of the Second Principal Factor.** With water as the first principal species, the second one should be obtained from the most concentrated sucrose solution utilized. However, because the  $991\text{ cm}^{-1}$  band intensity at 2.89 au for the 2.628 M sucrose solution (Figure 3) is close to the spectrum saturation limit for sucrose solutions, we chose to use the 2.337 M solution as the second principal species instead. This spectrum was subtracted from the other spectra in Figure 3. Starting from the lowest concentration, the residue spectra in the  $1000\text{ cm}^{-1}$  region (figure not presented) showed a regular pattern that increased with the sucrose concentration up to 1.168 M, whereupon further additions of sucrose caused the intensity of the pattern to decrease. We checked the residue spectra for a possible temperature effect<sup>36</sup> and found that the temperature variation of the solutions had very little effect on the spectra. We then decided to try FA with three factors.

**3.4. Factor Analysis Using Three Principal Spectra.** **3.4.1. Determination of a Third Principal Spectrum.** The first principal spectrum, that of pure water, is shown as trace a in Figure 4A. Trace c of the same figure is the spectrum of sucrose hydrate II and is the 2.337 M sucrose solution subtracted from its pure water spectrum; trace c constitutes the second principal spectrum. The third principal spectrum, shown as trace b in Figure 4A, was obtained from the 1.168 M sucrose solution spectrum by subtracting from it its pure water and sucrose hydrate II spectra. The resulting spectrum, normalized to 2.337 M sucrose, is that of sucrose hydrate I. The two sucrose species form hydrates because they contain different amounts of water. The two sucrose spectra are not orthogonal at this stage because each may contain some of the other as a contaminant. Fortunately, FA can be correctly executed with nonorthogonal spectra.<sup>25,27,29</sup>

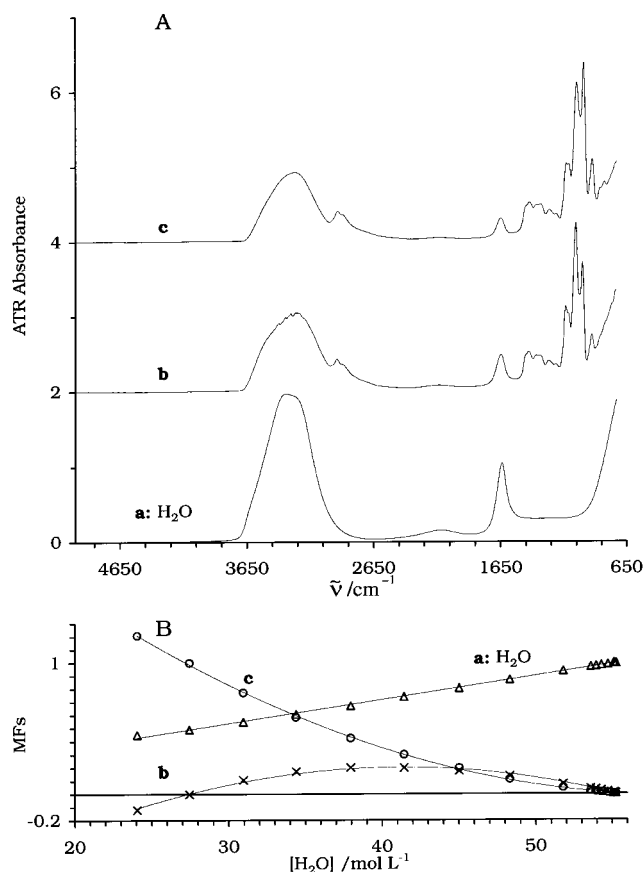


**Figure 4.** FA with three principal factors: pure water, a; sucrose hydrate I, b; sucrose hydrate II, c. (A) spectra, (B) MFs retrieved.

**3.4.2. FA Results.** The MFs resulting from FA using the three principal spectra of Figure 4A are presented in Figure 4B. The residues obtained from the differences between experimental and calculated spectra are given in Figure 5. Compared to the residues obtained with two principal spectra, those obtained with three principal spectra are smaller by a factor of 50. The residue intensity in the  $1000\text{ cm}^{-1}$  region is less than 1% of the most intense band of Figure 3, except for the 2.628 M sucrose solution where it is 2%. In the OH stretch and HOH deformation regions, the residues are at the same level as what is obtained with a  $0.3\text{ }^{\circ}\text{C}$  temperature variation.<sup>36</sup> This variation is the temperature stability limit of our spectrophotometric system.

Trials with more than three principal species did not significantly decrease the intensity residues. It was then concluded that three species—pure water and two sucrose hydrates—are sufficient to describe the entire series of 18 sucrose/water mixtures. One MF in Figure 4Bb is below the zero level and is not the result of experimental error. This is impossible since it would indicate that the concentration of one sucrose species is below zero. At this stage we must consider these principal factors as nonorthogonal. In section 3.5 we will show how to transform them into orthogonal factors.

The MFs of Figure 4B were transformed into concentrations and plotted in Figure 6A. The total sucrose and water concentrations were calculated and correlated with those obtained by gravimetry in Figures 6B and C, respectively. The excellent correlation of 0.999 indicates that the results are reliable and that the FA procedure is adequate. The use of two different sucrose hydrates has permitted us to use the IR measurements for the complete solubility range of sucrose, whereas the use of only one sucrose species led to a limited concentration range linearity.<sup>9,10,12,15</sup>



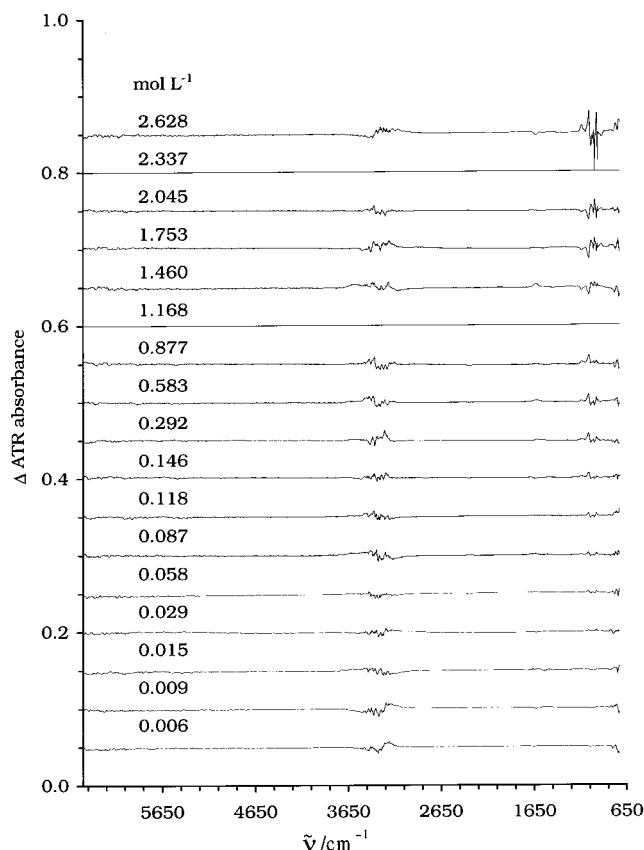


**Figure 5.** Residues spectra obtained from the difference between calculated ( $\Sigma$  (MF  $\times$  eigenspectrum)) and experimental (Figure 1) sucrose solution spectra. Same order as in Figure 1, successively displaced by 0.05 au. Note intensity scale is increased by a factor 20 compared to Figure 3.

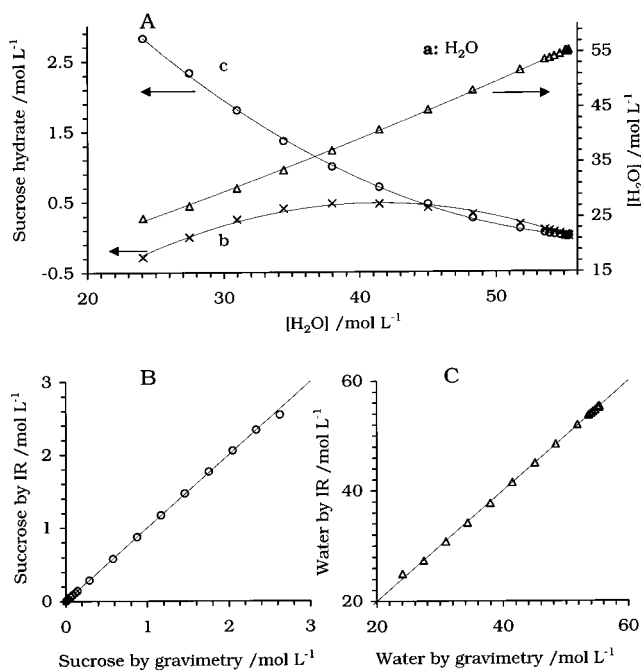


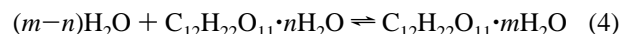
**Figure 6.** Species concentrations in the sucrose solutions. (A) Separate species: pure water, a ( $\Delta$ , right scale); sucrose hydrate I, b ( $\times$ , left scale); sucrose hydrate II, c ( $\circ$ , left scale). (Note the different scales for water and sucrose species.) Correlation between the concentration retrieved by IR and by gravimetry: (B) sucrose ( $\circ$ ) and (C), water ( $\Delta$ ).

**3.5. Real MFs and Spectra of Sucrose Hydrates.** Given that water and the sucrose hydrates I and II are the three

principal species present in the sucrose solutions, we can determine their hydration numbers and obtain their *real* orthogonal spectra through considerations of thermodynamic equilibrium.

**3.5.1. Thermodynamic Equilibrium in Aqueous Sucrose and Hydration Numbers.** The sucrose hydrates contain strongly hydrogen bonded water. Since the integrated intensity of the OH bands of aqueous sucrose is nonlinearly related to the water content of the species, it is not possible to use these bands to determine their hydration numbers. One way to surmount this impasse is to analyze the chemical equilibrium between the two hydrates.

The concentrations retrieved by IR of the three principal species present in aqueous sucrose are given in Figure 6A. The concentrations of the two sucrose species have been counted as sucrose equivalent (left scale). The two sucrose hydrates contain  $n$  and  $m$  water molecules for the high and low sucrose concentrations, respectively. The equilibrium between the hydrates is



and the equilibrium constant is

$$K_e = \frac{[\text{C}_{12}\text{H}_{22}\text{O}_{11} \cdot m\text{H}_2\text{O}]}{[\text{C}_{12}\text{H}_{22}\text{O}_{11} \cdot n\text{H}_2\text{O}][(\text{H}_2\text{O})]^{m-n}} \quad (5)$$

The spectral subtraction of water has overestimated the pure or “unperturbed” water content of the samples as almost equal to the total water present (Figure 6A,  $\Delta$ , right scale). Therefore, the amount of “unperturbed” water retrieved by FA using the pure water spectrum must be decreased in order that the values  $n$  and  $m$  concur. Equation 5 was applied to the concentrations retrieved by FA using several  $n$  and  $m$  values. For the set (0,0),  $K_e$  decreased with decreasing water concentration, indicating that the chosen set does not correctly corroborate the presence of water in the sucrose hydrates. With the set (2,5), the  $K_e$  obtained is shown in Figure 7A. No other combination of  $n$  and  $m$  values gave a flatter  $K_e$  curve than that presented in this figure. Since  $K_e$  is a constant, its proximity to a horizontal line is a criterion of correctness. From this result we gather that the sucrose species in aqueous solutions are made of sucrose dihydrates and pentahydrates.

In Figure 7A, the  $K_e$  values are very nearly constant at  $(1.1 \pm 0.1) \times 10^{-5} \text{ L}^3 \text{ mol}^{-3}$  for water concentrations between 34 and 53 mol/L. Outside this range we observe some deviation. Loss of linearity at the high end of the scale is attributable to the low sucrose concentrations, which greatly increases the error. Deviations on the left can be explained by the nonorthogonality of the sucrose hydrates as defined. A certain amount of each sucrose species may contaminate the other. This would explain the negative MFs ( $-0.12$ ) at 24.07 mol/L in Figure 4Bb. However, since orthogonal spectra are necessary for an adequate spectral analysis, we will show how they are obtained in the next section.

**3.5.2. Real MFs and Spectra of Sucrose Dihydrate and Pentahydrate.** The FA procedure applied to the 18 experimental spectra ( $\mathbf{S}^{\text{exp}}$ ) makes use of three principal spectra ( $\mathbf{S}^{\text{p}}$ ). These were obtained from a particular set of three experimental spectra ( $\mathbf{S}_p^{\text{exp}}$ ): pure water, and the 1.168 and 2.337 M sucrose solutions. The three data matrices ( $\mathbf{S}^{\text{exp}}$ ,  $\mathbf{S}^{\text{p}}$ ,  $\mathbf{S}_p^{\text{exp}}$ ), each having

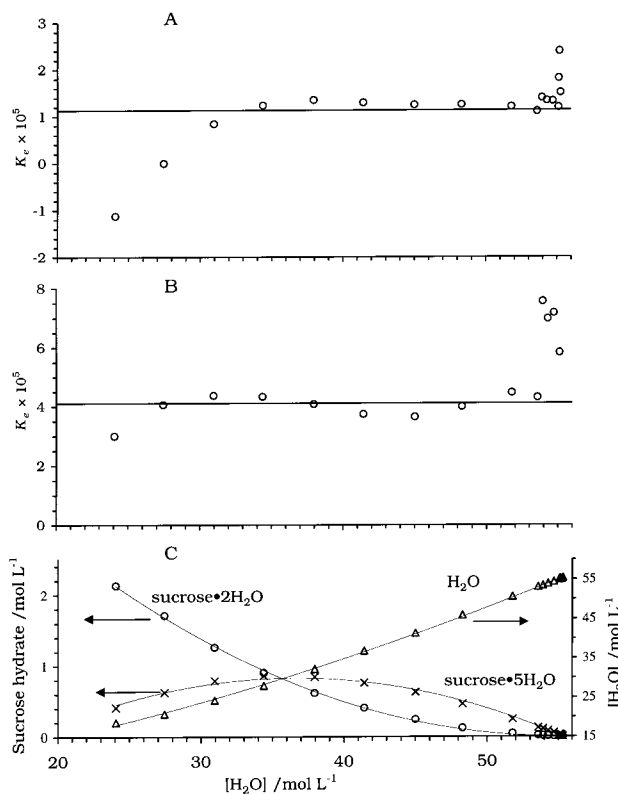


**Figure 7.** Equilibrium constant ( $K_e$ ) of sucrose di- and pentahydrate when the concentrations are calculated with (A) nonorthogonal spectra; (B) orthogonal spectra (see text). (C) Species concentrations in the sucrose solutions obtained from the orthogonal spectra: pure water ( $\Delta$ , right scale); sucrose pentahydrate ( $\times$ , left scale); and sucrose dihydrate ( $\circ$ , left scale). Note that the arrows point toward the ordinate giving the concentration scales of the different species.

$j$  columns ( $j$  is the number of spectral data points), are related through the expressions

$$\mathbf{S}^{\text{exp}} = \mathbf{MF} \times \mathbf{S}^{\text{P}} \quad (6)$$

$$\mathbf{S}^{\text{P}} = \mathbf{P} \times \mathbf{S}_p^{\text{exp}} \quad (7)$$

where  $\mathbf{MF}$  is the matrix of the MFs of the experimental spectra (Figure 4B) and  $\mathbf{P}$  is the matrix defining the principal spectra (Figure 4A) from the set of corresponding experimental spectra (same number of spectra).

Let ( $\mathbf{S}^{\text{P}'}$ ) be another set of principal spectra differently obtained from the same set of three experimental spectra ( $\mathbf{S}_p^{\text{exp}}$ ). Relations similar to eqs 6 and 7 are obtained:

$$\mathbf{S}^{\text{exp}} = \mathbf{MF}' \times \mathbf{S}^{\text{P}'} \quad (8)$$

$$\mathbf{S}^{\text{P}'} = \mathbf{P}' \times \mathbf{S}_p^{\text{exp}} \quad (9)$$

where  $\mathbf{MF}'$  and  $\mathbf{P}'$  correspond to  $\mathbf{MF}$  and  $\mathbf{P}$  of eqs 6 and 7.

Combining eqs 6 and 7, one obtains

$$\mathbf{S}^{\text{exp}} = \mathbf{MF} \times \mathbf{P} \times \mathbf{S}_p^{\text{exp}} \quad (10)$$

Taking the inverse of eq 9 yields

$$\mathbf{P}'^{-1} \times \mathbf{S}^{\text{P}'} = \mathbf{S}_p^{\text{exp}} \quad (11)$$

Combining eqs 10 and 11, one obtains

$$\mathbf{S}^{\text{exp}} = \mathbf{MF} \times \mathbf{P} \times \mathbf{P}'^{-1} \times \mathbf{S}^{\text{P}'} \quad (12)$$

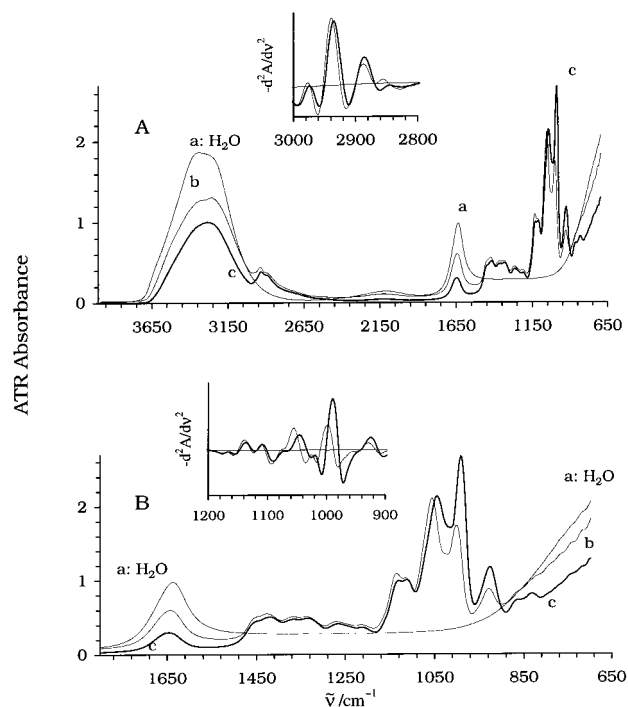


**Figure 8.** ATR-IR orthogonal spectra in the sucrose solutions:  $\text{H}_2\text{O}$ , a; sucrose pentahydrate normalized to 2.337 M, b; sucrose dihydrate normalized to 2.337 M, c. (A) 4000–650  $\text{cm}^{-1}$  (inset, second derivative of the C–H bands); (B) 1800–650  $\text{cm}^{-1}$  regions (inset, second derivative of the C–O bands).

Comparing eqs 8 and 12 leads to

$$\mathbf{MF}' = \mathbf{MF} \times \mathbf{P} \times \mathbf{P}'^{-1} \quad (13)$$

Equation 13 indicates that replacing the set of principal spectra ( $\mathbf{S}^{\text{P}}$ ) by another set ( $\mathbf{S}^{\text{P}'}$ ) obtained from the same set of experimental spectra ( $\mathbf{S}_p^{\text{exp}}$ ), (same number of spectra as the principal species), and replacing the MFs by values obtained via eq 13 will result in exactly the same residues as in Figure 5. Therefore, after modifying the principal spectra that represent the pure sucrose dihydrate and pentahydrate, there is no need to perform the complete FA procedure again.

Oversubtracting the 2.337 M sucrose spectrum from the 1.168 M one lowered the absorption near 961  $\text{cm}^{-1}$  too much (Figure 4Ab). To correct for this, the subtraction was fine-tuned with the second derivative spectra in the 1010–940  $\text{cm}^{-1}$  range, where the strongest absorption bands occur. By considering an ideal ratio ( $r$ ) between maximum and minimum in the second derivative spectrum, a sucrose hydrate II MF of 0.238 was subtracted from the 1.168 M sucrose spectrum to obtain the spectrum for sucrose pentahydrate. This spectrum normalized to 2.337 M is presented in traces b of Figure 8.

The same procedure could not be used for the sucrose dihydrate spectrum. Instead we used the equilibrium eqs 4 and 5. The subtraction of the pentahydrate spectrum from that of the 2.337 M sucrose solution was adjusted to a constant  $K_e$  between 24 and  $\sim 54$  M water. The result is presented in Figure 7B where the full line represents  $K_e = (4.1 \pm 0.3) \times 10^{-5} \text{L}^3 \text{mol}^{-3}$ . This value is valid over the range 27 to  $\sim 54$  M water ( $\sim 0.1$  to 2.34 M sucrose). Outside this region the sucrose spectra were not reliable either because of a low signal-to-noise ratio ( $< 0.1$  M sucrose) or because of the intensity saturation ( $> 2.4$  M sucrose). The spectrum of sucrose dihydrate normalized to 2.337 M is presented in Figure 8c and the real MFs in Table 1.

**TABLE 2: Band Positions (in cm<sup>-1</sup>) of Aqueous Sucrose**

assignment <sup>a</sup>	Kodad et al. <sup>5</sup>		this work		
	solid sucrose	aqueous sucrose	sucrose dihydrate	sucrose pentahydrate	H <sub>2</sub> O
$\nu_3$ H <sub>2</sub> O + $\nu$ OH			~3290	~3350	3389 <sup>b</sup>
$\nu_1$ H <sub>2</sub> O + $\nu$ OH			~3240	~3240	3222 <sup>b</sup>
$\nu$ CH <sub>3</sub> as			2970	2974	
$\nu$ CH <sub>2</sub> as			2933	2938	
$\nu$ CH <sub>2</sub> s			2880	2882	
comb.			2843	2850	
comb.			2680	2680	
comb.			~2500	~2500	
$\nu_2 + \nu_L$ H <sub>2</sub> O			~2125	~2125	2115
$\nu_2$ H <sub>2</sub> O		1640	1648	1645	1638
	1461				
		1451	1452	1454	
$\delta$ C—O—H <sup>K</sup>	1431	1430	1420	1425	
	1410				
$\delta$ C—O—H glu <sup>K</sup>	1370	1366	1370	1370	
$\delta$ C—O—H fru <sup>K</sup>	1346	1336	1331	1333	
	1323				
	1280				
$\omega$ CH <sub>2</sub> <sup>K</sup>		1265	1270	1275	
$\tau$ CH <sub>2</sub> <sup>K</sup>	1239	1247			
			1210	1210	
	1162				
$\nu$ C—O endo fru <sup>K</sup>	1130	1136	1132	1135	
$\nu$ C—O endo glu <sup>K</sup>	1106	1113	1110	1113	
	1069				
$\nu$ C—O exo <sup>K</sup>	1052	1055	1045 vs	1055 vs	
	1008				
$\delta$ C—O—H <sup>K</sup>	990	993	993 vs	998 vvs	
$\nu$ C—C glu <sup>K</sup>	941	945			
$\nu$ C—C fru <sup>K</sup>	911	925	928	929	
$\nu$ C—C <sup>K</sup>	867	870	868	868	
	849				
$\delta$ (C <sub>2</sub> —C <sub>1</sub> —H) glu <sup>K</sup>		835			
$\delta$ (C <sub>3</sub> —C <sub>2</sub> —H) fru <sup>K</sup>		828	830		

<sup>a</sup> The water bands are identified by H<sub>2</sub>O; the other bands are those of sucrose. The assignments made by Kodad et al.<sup>5</sup> are identified by superscript K. The following notation also applies: fru, D-fructosyl moiety; glu, D-glucosyl moiety;  $\delta$ , deformation;  $\nu$ , stretch;  $\tau$ , torsion;  $\omega$  wag; endo, endocyclic; exo, exocyclic. <sup>b</sup> Obtained by Gaussian band fitting.

In this table we note that none of the MFs are below the zero level, which indicates that the procedure of rendering the Figure 4B MFs real is suitable. These MFs transformed into concentrations are presented in Figure 7C where no species concentration is below the zero mark. On this figure starting at the high water concentration level (low sucrose concentration, right side), the concentration of pure water decreases almost linearly as the sucrose concentration increases. Following the same concentration direction, sucrose pentahydrate starts at the zero level (right side), reaches a plateau at 38–34 M H<sub>2</sub>O (1.46–1.75 M sucrose), and decreases thereafter (Table 1). Sucrose dihydrate starts at the zero level (right side), increases slowly following a second-order curve, crosses the pentahydrate curve at its plateau, and continues moving up as the sucrose concentration increases (left side).

**3.6. Spectral Features of Sucrose Hydrates in Water.** **3.6.1. Comparison between Aqueous Sucrose Dihydrate and Pentahydrate.** The spectra of pure sucrose dihydrate and pentahydrate (both normalized to 2.337 M sucrose) are shown in Figure 8 along with the spectrum of pure water. The assignment of the bands is made in Table 2. Both hydrate spectra are very similar, having bands at almost the same places with similar intensities in all but a few places. The second derivative spectra were used

to enhance the differences between the two hydrates where that proved useful (insets in Figure 8).

In the second-derivative spectra of the C—H region (3000–2800 cm<sup>-1</sup>, inset Figure 8A) a difference of less than 5 cm<sup>-1</sup> is observed between the two principal bands; intensity differences are minimal. This result indicates that the sucrose CH groups are similar in the two hydrates. The H—C—H and H—O—C deformation bands in the 1500–1190 cm<sup>-1</sup> (Figure 8B) show only a small intensity difference due to the amount of associated water in the two hydrates.

The bands in the 1000 cm<sup>-1</sup> region were enhanced by the second-derivative technique (Fig. 8B, inset). The position of the bands is not much different in the two hydrates: the pentahydrate 1055 and 998 cm<sup>-1</sup> bands are displaced in the dihydrate to 1045 and 993 cm<sup>-1</sup>, respectively. The other band displacements in this region are within the resolution limit. The greatest differences in this region are observed in the intensity of the 995 (998 and 993 cm<sup>-1</sup> for the pentahydrate and dihydrate, respectively) and the 929 cm<sup>-1</sup> bands. The two bands are more intense in the dihydrate (c) than in the pentahydrate (b) (Figure 8B). The slight difference in intensity in the other bands is mainly due to differences in water content in the two species because the far wing of the water libration bands ( $\nu_{\max}$  at 613 cm<sup>-1</sup>)<sup>34</sup> that starts to absorb near 1100 cm<sup>-1</sup> influences the two species differently. It is the difference in intensity between the 995 and 929 cm<sup>-1</sup> bands that has allowed us to separate the spectra of the two sucrose species.

The other big differences in the spectra of the sucrose solution species involve the OH groups. The  $\nu_{\text{OH}}$  band near 3300 cm<sup>-1</sup> is assigned to the OH stretch of water and sucrose. This band is situated near 3340 cm<sup>-1</sup> in water and is displaced to near 3260 cm<sup>-1</sup> in the dihydrate with a corresponding intensity decrease and band shape modifications (Figure 8A). The HOH deformation band passes from 1638 cm<sup>-1</sup> in pure water to 1645 cm<sup>-1</sup> in the pentahydrate and to 1648 in the dihydrate (Figure 8B). This band shows a nonlinear intensity decrease from pure water to the dihydrate (Figure 2A, right scale), although this band is entirely due to water. The nonlinear intensity relationship observed on the different types of water is discussed in the next section.

**3.6.2. Calculated Integrated Intensities in Aqueous Sucrose.** The three species present in the aqueous sucrose solution contain some OH groups that contribute to the total OH stretching band intensity. The OH stretch molar integrated intensity contribution of pure water was obtained from its IR spectrum (Figure 4A) and was evaluated to be  $\int_{\nu_{\text{OH}}}^{\text{pure water}} I(\nu) d\nu = 852/(55.35 \times 2) = 7.70 \text{ au} \times \text{cm}^{-1}/(\text{mol OH}) \text{ L}^{-1}$ . In another study on mixtures of ordinary water and heavy water, this value was the same and was found to remain constant over the complete range of H<sub>2</sub>O and D<sub>2</sub>O mixtures (unpublished results). Consequently, the variation that was observed on the OH stretch band of aqueous sucrose must be due to another mechanism, namely the associated water and the sucrose OH.

The concentration of each species is given in Figure 7C so that the total integrated OH intensity of the samples can be evaluated by the following relationship:

$$\int_{\nu_{\text{OH}}}^{\text{sample}} I(\nu) d\nu = c_{\text{pw}} \int_{\nu_{\text{OH}}}^{\text{pure water}} I(\nu) d\nu + c_{\text{d}} \int_{\nu_{\text{OH}}}^{\text{sucrose dihydrate}} I(\nu) d\nu + c_{\text{p}} \int_{\nu_{\text{OH}}}^{\text{sucrose pentahydrate}} I(\nu) d\nu \quad (14)$$

where  $c_{\text{pw}}$  and  $\int_{\nu_{\text{OH}}}^{\text{pure water}} I(\nu) d\nu$ ,  $c_{\text{d}}$  and  $\int_{\nu_{\text{OH}}}^{\text{sucrose dihydrate}} I(\nu) d\nu$ , and



$c_p$  and  $\int_{\nu_{OH}}^{\text{sucrose pentahydrate}} I(\nu) d\nu$  are the concentration and contribution to the  $\nu_{OH}$  intensity of pure water, sucrose dihydrate, and sucrose pentahydrate, respectively. The OH stretch molar integrated intensities of both sucrose hydrates were evaluated from spectra in Figure 8: 443/2.337 and 602/2.337  $\text{au} \times \text{cm}^{-1}/\text{mol L}^{-1}$  for the di- and pentahydrate, respectively. With the use of eq 14, calculations were made for each sample with the concentrations retrieved by FA (Figure 7C). The results, which are plotted by the full line (left scale) in Figure 2A, are close to the experimental values ( $\circ$  symbols). Calculations were also performed to determine the HOH deformation integrated intensity; the values calculated (Figure 2A, full line, right scale) were close to those found experimentally ( $\Delta$  symbols). The integrated intensities calculated with the new set of concentrations, which fall on the experimental values indicate that the concentrations retrieved, are reliable.

**3.6.3. Individual Contributions to the Aqueous Sucrose  $\nu_{O-H}$  Integrated Intensity.** Sucrose has 8 OH groups. Since sucrose dihydrate and pentahydrate have 12 and 18 OH groups, respectively, the mean integrated  $\nu_{OH}$  intensity per OH  $\text{mol L}^{-1}$  is 14.3 and 15.8  $\text{au} \times \text{cm}^{-1}/(\text{mol OH}) \text{L}^{-1}$  for sucrose pentahydrate and dihydrate, respectively. These intensities are nearly twice that obtained in pure water (7.7  $\text{au} \times \text{cm}^{-1}/(\text{mol OH}) \text{L}^{-1}$ ). Extrapolating the quadratic tendency exhibited by the mean OH stretch molar integrated intensity against water concentration (Figure 2C,  $\circ$  symbols, left scale) to 0.0 M  $\text{H}_2\text{O}$  yields 15.9  $\text{au} \times \text{cm}^{-1}/(\text{mol sucrose OH}) \text{L}^{-1}$ , a value more than twice its pure water value (7.7  $\text{au} \times \text{cm}^{-1}/\text{mol L}^{-1}$ ). A similar result was observed in 1-propanol.<sup>37</sup> Unlike sucrose, 1-propanol can be studied as a pure liquid. If we suppose that the mean contribution of a sucrose OH group is 15.9  $\text{au} \times \text{cm}^{-1}/(\text{mol sucrose OH}) \text{L}^{-1}$  for both hydrates, we can evaluate the contribution of the bonded water molecules. The results are 15.5 (= [443 - (8 × 15.9 × 2.337)]/[2.337 × 2 × 2]) and 13.0 (= [602 - (8 × 15.9 × 2.337)]/[2.337 × 5 × 2])  $\text{au} \times \text{cm}^{-1}/(\text{mol water OH}) \text{L}^{-1}$  in sucrose dihydrate and pentahydrate, respectively. These results indicate that the water OH intensity is nearly doubled when water is hydrogen-bonded to sucrose. More experimental work on a variety of bound-water systems is needed to substantiate these results.

#### 4. Conclusion

An aqueous sucrose solution is made up of three species: pure water; pentahydrate ( $\text{C}_{12}\text{H}_{22}\text{O}_{11} \cdot 5 \text{H}_2\text{O}$ ); and dihydrate ( $\text{C}_{12}\text{H}_{22}\text{O}_{11} \cdot 2 \text{H}_2\text{O}$ ). The abundances of these species were determined as a function of water concentration. The equilibrium constant between the two hydrates was found to be  $(4.1 \pm 0.3) \times 10^{-5} \text{L}^3 \text{mol}^{-3}$ . We found no evidence of a monohydrate, although this possibility cannot be ruled out given our limited results near saturation where this species could exist.

The IR spectra of both sucrose hydrates were obtained in the 6000–700  $\text{cm}^{-1}$  range. Both spectra are similar except for a few limited regions. In the intense C–O stretch region near 1000  $\text{cm}^{-1}$ , two bands situated near 1050 and 995  $\text{cm}^{-1}$  have different intensities in the two hydrates, while the other bands in that region present small intensity variations. The positions of all the bands in this region are displaced but very little. The water HOH deformation band is blue shifted slightly in the hydrates: from the pure water position it is displaced 7 and 10  $\text{cm}^{-1}$  in the penta- and dihydrate, respectively. Its molar integrated intensity is increased in passing from pure water to the dihydrate. The OH stretch band is red shifted in passing from pure water to the dihydrates (80  $\text{cm}^{-1}$ ), with an increase in intensity and a change in shape. Compared to that in pure

liquid water, the  $\nu_{O-H}$  molar integrated intensity of water bound to sucrose in the hydrate is multiplied by a factor of 2. This intensity is close to that obtained for the mean contribution of the sucrose OH groups and is almost equal to that of the alcoholic OH group found in 1-propanol.<sup>37</sup>

The use of the spectra of the two sucrose hydrates present in aqueous sucrose solutions have permitted us to extend the analytical range of IR spectroscopy to the concentration range 0–900  $\text{g L}^{-1}$  (2.63  $\text{mol L}^{-1}$ ), which is almost at the saturation limit. A normal coordinate analysis of both sucrose hydrates could help in determining the organization of the water molecules bound to the hydrates.

**Acknowledgment.** M. Trudel and F. Carlot helped in taking the IR spectra.

#### References and Notes

- (1) Scatchard, G. *J. Am. Chem. Soc.* **1921**, *43*, 2406.
- (2) Sugden, J. N. *J. Chem. Soc.* **1926**, 129, 174.
- (3) Immel, S.; Lichtenthaler, F. W. *Liebigs Ann.-Chem.* **1995**, *11*, 1925.
- (4) Lichtenthaler, F. W.; Pokinskyj, P.; Immel, S. *Zuckerindustrie* **1996**, *121*, 174.
- (5) Kodad, H.; Mokhlisse, R.; Davin, E.; Mille, G. *Can. J. Appl. Spectrosc.* **1994**, *39*, 107.
- (6) Back, D. M.; Michalska, D. F.; Polavarapu, P. L. *Appl. Spectrosc.* **1984**, *38*, 173.
- (7) Polavarapu, P. L.; Chatterjee, S. R.; Michalsk, D. F. *Carbohydr. Res.* **1985**, *137*, 253.
- (8) Mirouze, F. D. L.; Boulou, J. C.; Dupuy, N.; Meurens, M.; Huvenne, J.-P.; Legrand, P. *Appl. Spectrosc.* **1993**, *47*, 1187.
- (9) Lendl, B.; Kellner, R. *Mikrochim. Acta* **1995**, *119*, 73.
- (10) Cadet, F.; Robert, C.; Offman, B. *Appl. Spectrosc.* **1997**, *51*, 369.
- (11) Lendl, B.; Schindler, R.; Frank, J.; Kellner, R.; Drott, J.; Laurell, T. *Anal. Chem.* **1997**, *69*, 2877.
- (12) Kameoka, T.; Okuda, T.; Hashimoto, A.; Noro, A.; Shiinoki, Y.; Ito, K. *J. Japan Soc. Food Sci. Technol.* **1998**, *45*, 199.
- (13) Schindler, R.; Watkins, M.; Vonach, R.; Lendl, B.; Kellner, R.; Sara, R. *Anal. Chem.* **1998**, *70*, 226.
- (14) Cadet, F. *Talanta* **1999**, *48*, 867.
- (15) Hashimoto, A.; Kameoka, T. *Appl. Spectrosc.* **2000**, *54*, 1005.
- (16) Kislina, I. S.; Maiorov, V. D.; Librovich, N. B.; Vinnik, M. I. *Rus. J. Phys. Chem.* **1976**, *50*, 1676.
- (17) Max, J.-J.; Chapados, C. *Appl. Spectrosc.* **1999**, *53*, 1045.
- (18) Max, J.-J.; Trudel, M.; Chapados, C. *Appl. Spectrosc.* **1998**, *52*, 234.
- (19) Max, J.-J.; Chapados, C. *Appl. Spectrosc.* **1999**, *53*, 1601.
- (20) Max, J.-J.; Chapados, C. *Appl. Spectrosc.* **1998**, *52*, 963.
- (21) Max, J.-J.; Chapados, C. *Can. J. Chem.* **2000**, *78*, 64.
- (22) Max, J.-J.; Trudel, M.; Chapados, C. *Appl. Spectrosc.* **1998**, *52*, 226.
- (23) Baril, J.; Max, J.-J.; Chapados, C. *Can. J. Chem.* **2000**, *78*, 490.
- (24) Max, J.-J.; Ménéchelli, C.; Chapados, C. *J. Phys. Chem. A* **2000**, *104*, 2845.
- (25) Max, J.-J.; Chapados, C. *J. Chem. Phys.* **2000**, *113*, 6803.
- (26) Ménéchelli, C.; Max, J.-J.; Chapados, C. *Can. J. Chem.* **2000**, *78*, 1128.
- (27) Max, J.-J.; Blois, S. d.; Veilleux, A.; Chapados, C. *Can. J. Chem.* **2001**, *79*, 13.
- (28) Zhao, Z.; Malinowski, E. R. *Anal. Chem.* **1999**, *71*, 602.
- (29) Max, J.-J.; Chapados, C. *J. Chem. Phys.* **2001**, *115*, 2664.
- (30) Wieliczka, D. M.; Weng, S.; Querry, M. R. *Appl. Opt.* **1989**, *28*, 1714.
- (31) Malinowski, E. R.; Howery, D. G. *Factor analysis in chemistry*; Robert E Krieger Publishing Co: Malabar, FL, 1989.
- (32) Chapados, C.; Trudel, M. *Biophys. Chem.* **1993**, *47*, 267.
- (33) Savitzky, A.; Golay, M. J. E. *Anal. Chem.* **1964**, *36*, 1627.
- (34) Zelsmann, H. R. *J. Mol. Struct.* **1995**, *350*, 95.
- (35) Weast, R. C. *Handbook of Chemistry and Physics*, 57th ed; CRC Press: Cleveland, 1976.
- (36) Iawata, T.; Koshoubu, J.; Jin, C.; Okubo, Y. *Appl. Spectrosc.* **1997**, *51*, 1269.
- (37) Max, J.-J.; Daneault, S.; Chapados, C. *Can. J. Chem.* **2001**, in press.